Impurities in Hydride Gases Part 1: Investigation of Trace Moisture in the Liquid and Vapor Phase of Ultra-Pure Ammonia by FTIR Spectroscopy

HANS H. FUNKE,[1] MARK W. RAYNOR,[1] BELGIN YÜCELEN,[1] and VIRGINIA H. HOULDING[1,2]

1.—Matheson Tri-Gas, Advanced Technology Center, 1861 Lefthand Circle, Longmont, CO 80501. 2.—e-mail: vhoulding@matheson-trigas.com, Fax: 303-442-0711

Trace moisture in ammonia is a critical impurity in the growth of epitaxial nitride films. Because moisture is very soluble in the liquid phase of ammonia, moisture in the vapor phase increases dramatically with cylinder use, and is often far higher than the nominal purity specification. A reliable method was developed for sampling and analyzing trace moisture in both liquid- and vapor-phase ammonia using FTIR. Analysis of liquid-phase ammonia gives a stable and representative moisture value whereas gas-phase moisture levels strongly depend on sampling time, flow rate, temperature, mixing, and extent of cylinder use. The variation of vapor-phase moisture is discussed in terms of a variable vaporization model with applications to high flow.

Key words: Moisture, impurities, ammonia, partition coefficient, FTIR spectroscopy, liquid phase delivery, gas phase, thermodynamic equilibrium

INTRODUCTION

The purity of process-specialty gases is critical to success in the manufacture of epitaxial films and micro-electronic integrated-circuit devices.[1] Many processes are sensitive to gas impurities on the level of parts per billion (ppb). Gases used for semiconductor device manufacturing must be rigorously free of trace impurities that will alter the processes. Thus, the ability to measure trace impurities at the ppb level is very important in the manufacture of electronic-grade specialty gases.

Ultra-high purity-grade ammonia is currently used for metalorganic chemical vapor deposition (MOCVD) growth of GaN films in the production of blue light-emitting diodes (LEDs) and the new high-speed devices. The performance of the LEDs is strongly dependent on the purity of the precursors. Moisture in particular appears to decrease the performance,[2] and most compound semiconductor manufacturers prefer ammonia with a moisture specification of less than 2 parts per million (ppm). As a result, various analytical techniques for monitoring moisture in ammonia have been investigated by several groups for potential applications in production quality control and in-situ real-time monitoring of gas delivery systems.

(Received June 5, 2001; accepted August 10, 2001)

BACKGROUND OF THE ANALYTICAL PROBLEM

Ammonia and water have similar molecular weights, electronic structures, and polarities, making the analysis of trace moisture in ammonia very difficult by standard techniques such as mass spectrometry (MS) or gas chromatography (GC).[3] Sensors that are based on P_2O_5 electrolytic cells are chemically not compatible with ammonia. Reactive matrix-coated microbalance sensors can detect moisture in ammonia at the low ppb level[4,5] but have a limited dynamic range. Semiconductor Equipment and Materials International (SEMI) have approved a chemical method involving the catalytic decomposition of ammonia to nitrogen and hydrogen at 1000°C. Water passes over the catalyst unchanged and is determined using a commercial dew point moisture analyzer that can be operated in the inert N_2/H_2 matrix.[6] Unfortunately, the method detection limit of ~3 ppm is not sufficient

for current purity requirements. Other traditional methods of moisture determination, such as the Karl-Fischer moisture technique, cannot be applied in the presence of ammonia.[1] Analysis of water residuals after evaporation of the matrix ammonia is possible but water losses during the evaporation process limit the accuracy to several ppm.

Infrared absorption methods, such as Fourier transform infrared spectroscopy (FTIR) and near infrared tunable diode laser spectroscopy (NIR-TDL), are sensitive, rapid, non-destructive, and allow direct gas-phase analysis. The infrared spectra of water and ammonia overlap throughout the spectral range (Fig. 1), so the key to high sensitivity is careful compensation for ammonia interference.[7-9] NIR-TDL potentially is more sensitive than FTIR because of the high light intensity and a spectral resolution of ~0.001 cm^{-1}. However, despite advances in this technique, NIR-TDL has not gained widespread acceptance, mainly because of cost, complexity, reliability issues, and a lack of availability of commercial instruments.[10] Even though it is not as sensitive as NIR-TDL, reliable FTIR instruments are commercially available, and have been shown to be very suitable for trace gas analysis. Since FTIR spectrometers collect spectral information over a broad energy range, other impurities that absorb infrared light can be analyzed at the same time.[11] FTIR spectroscopy is more immune than NIR-TDL spectroscopy to chemical- or pressure-induced changes in the absorption spectrum, which could easily degrade the sensitivity and reproducibility of the system.

A number of research laboratories have recently investigated the use of FTIR for measurement of trace moisture in specialty gases. In the case of HCl and HBr, researchers have shown that detection limits of 10–30 ppb are possible.[12-14] In these gases, the moisture absorption region is well removed from the absorption bands of the matrix gas. In the case of the hydride gases (ammonia, arsine, and phosphine), Salim and coworkers pioneered FTIR analysis of moisture using an InSb detector, a Ge-coated KBr beamsplitter, and a standard 10 m White cell.[15,16] The spectral region >3600 cm^{-1} (where ammonia interference is weakest) was selected for moisture measurements. Data analysis was performed with a classical least-squares method to obtain detection limits of less than 10 ppb when the system operated optimally. The signal-to-noise ratio was found to be highest at a resolution of 4 cm^{-1}, enabling the use of an inexpensive low-resolution FTIR spectrometer for the analysis.

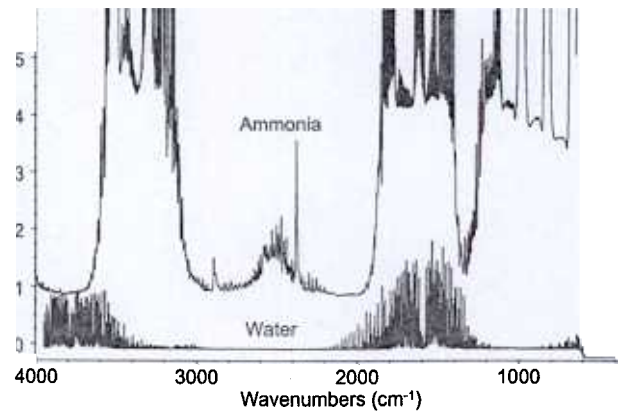

Fig. 1. Absorption spectra of ammonia and water in the mid-IR region.

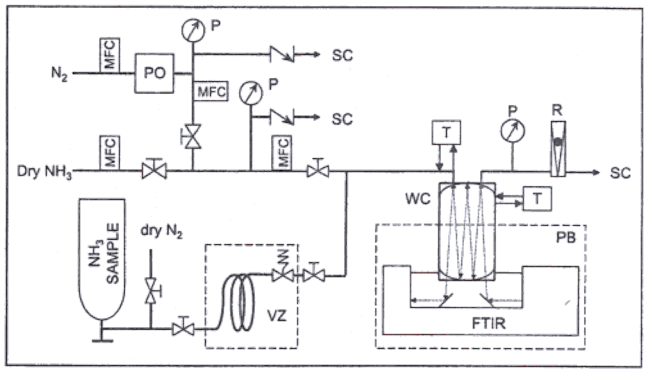

Fig. 2. Experimental setup for FTIR calibration and for liquid phase and vapor phase sampling of ammonia cylinders (PO—permeation oven; SC—scrubber; R—rotameter; MFC—mass flow controller; VZ—vaporization zone; WC—10-m pathlength White cell; PB—dry N_2 purge bag; T—temperature controller; P—pressure gauge.

The measurement of moisture at sub-ppm levels requires careful optimization of the hardware design, FTIR detector, operating parameters, and data analysis method. The following issues are particularly important. A long path length cell, such as a White cell (multi reflections of the light beam between two mirrors to increase the length of the light path) is required for high sensitivity because the magnitude of absorption is a function of the number of gas molecules in the light path (Beer's law) and the molecular density in the gas phase at ambient pressure is low. It is important to ensure that the cell is constructed of materials compatible with the gas to be tested to avoid degradation of the seals, mirrors, and windows during sampling and to prevent slow moisture equilibration times due to hygroscopic corrosion products. Additionally, heat tracing is recommended for dry-down within a few minutes to sub-ppm levels and to minimize moisture adsorption on the cell walls during sampling that could cause instabilities in the readings. A high sensitivity detector, such as liquid nitrogen-cooled mercury cadmium telluride (MCT) or indium antimonide (InSb), should be used. Minimization of atmospheric moisture in the spectrometer-beam path is required, either via a sealed bench or via a purge system, that utilizes purified inert gas with <1 ppb moisture levels. The absolute concentration of moisture in the bench is less critical since it is accounted for by background measurements prior to an experimental run. The short time-stability of the background, however, will be an important factor in the ultimate sensitivity, since background fluctuations during the experiment cannot be accounted for.

Several factors regarding data acquisition parameters affect the sensitivity. For example increasing

the number of IR scans that are averaged for each data point increases sampling time but decreases the spectral noise as a function of the square root of scan numbers. Lower resolution has been shown to minimize noise with an optimum around 4 cm^{-1}. Spectral apodization to minimize spectral artifacts from the Fourier transform at lower spectral resolution is typically applied but does not affect quantification if all calibration and sampling spectra are collected at identical conditions. Finally, the choice of a suitable data analysis method, such as a multivariate technique (classical least squares), adds to the precision of the analysis.[7]

The aim of our work has been the development of a sensitive, reliable, and rugged FTIR method that can be successfully utilized for routine measurement of moisture in ammonia in the low ppb range. While the initial development work of Salim and coworkers concentrated on the development and optimization of the FTIR instrumental parameters, it did not deal with issues involving calibration (which was performed in nitrogen rather than ammonia) and gas sampling. We have, therefore, focused not only on the FTIR methodology, but also on calibration and sampling issues. In our work, we encountered serious problems with repeatability and stability of gas-phase sampling of ammonia cylinders. We therefore developed a reliable liquid-phase sampling procedure that is described herein.

EXPERIMENTAL SECTION

FTIR Spectroscopy

A Nicolet Magna 750 FTIR bench (Nicolet Instruments, Madison, WI) equipped with a liquid-nitrogen-cooled MCT detector and a germanium-coated KBr beam splitter was used for moisture measurements. The bench was modified with additional internal purge lines and enclosed in an external purge bag to assure low and constant background moisture levels in the beam path. The spectrometer was purged at 20 slpm with purified nitrogen. The purified nitrogen purge gas was supplied from a bulk liquid source and dried with an in-line Nanochem® purifier (Semi Gas Systems, San Jose, CA) to less than 0.1 ppb

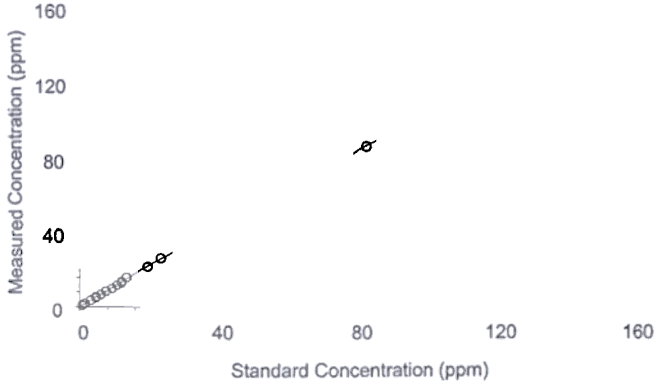

Fig. 3. Experimental calibration curve for moisture in ammonia matrix using classical least squares method.

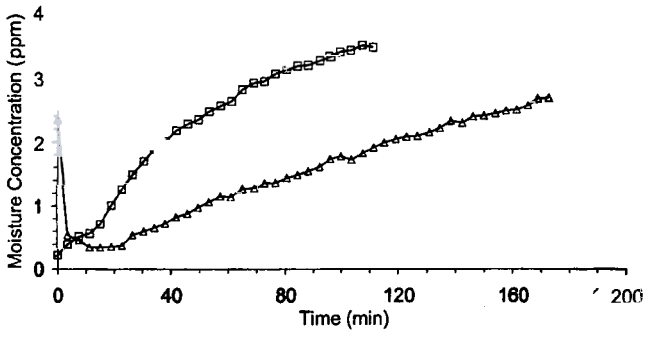

Fig. 4. Typical profiles of gas phase sampling of an ammonia cylinder (Liquid phase moisture = 35.7 ppm) at flow rates of 2 slpm (Δ) and 6 slpm (□).

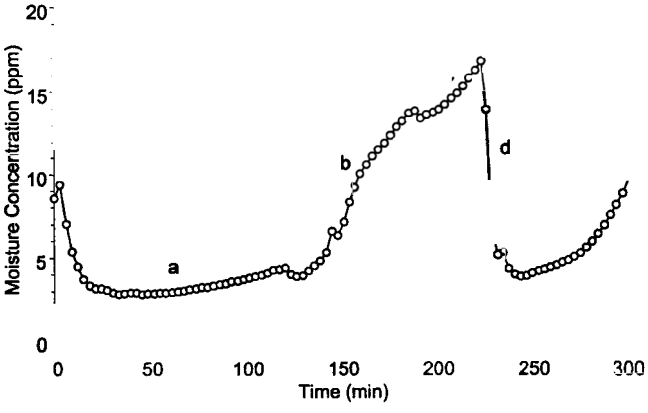

Fig. 5. Vapor phase sampling of an ammonia cylinder ($[H_2O]_{liquid}$ = 113 ± 0.7 ppm) at different flow rates: (a) 0.8 slpm; (b) 2 slpm; (c) 0.8 slpm; and (d) effect of agitation of the cylinder at 0.8 slpm.

moisture [as verified by atmospheric pressure ionization mass spectrometry (APIMS)]. A temperature controlled 10-m path-length nickel-coated aluminum White cell with gold-coated mirrors and IR quartz windows (Nicolet) was used for gas sampling. The gas inlet temperature was adjusted to match the cell wall temperature by controlling the heating rate of the inlet line based on the gas temperature at the cell inlet. The cell and gas inlet temperatures were maintained at 323 K for all measurements. The pressure in the FTIR cell was monitored with a Baratron pressure gauge (0–1000 torr) (MKS Instruments, Andover, MA) and was maintained near ambient pressure. Sampling was performed at a resolution of 4 cm^{-1} using Happ-Genzel apodization. 300 scans were co-added to obtain each infrared spectrum.

Sampling Procedure

The schematic in Fig. 2 illustrates the experimental setup used for gas-phase and liquid-phase sampling of ammonia cylinders as well as for instrument calibration. Metal-seated Titan II valves (Parker, Belleville, NJ) and heated 1/8″ electropolished 316 stainless steel lines were used for all connections except the CGA 660 teflon-sealed cylinder fittings to minimize adsorption-desorption of moisture. The gas flow through the cell was adjusted with an all-metal metering valve (Nupro, Willoughby, OH) and mea-

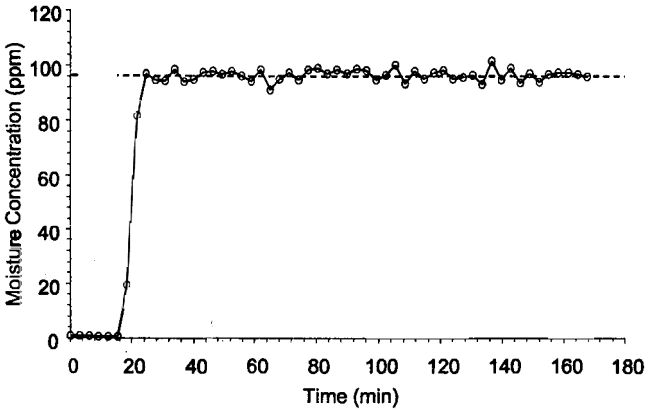

Fig. 6. Liquid phase sampling of an ammonia cylinder. Flow rate: 2 slpm.

sured with a rotameter at the exit of the FTIR cell.

A separately controlled heating zone between the cylinder valve and the metering valve was used to accomplish gas and liquid sampling with the same experimental setup. For gas-phase sampling, the cylinder was mounted in an upright position and the heated zone was maintained at a temperature close to that of the rest of the line. For liquid-phase sampling, the cylinders were mounted upside down with a custom-made cylinder inverter and the separately heated line segment was heated above 130°C to instantaneously and completely vaporize the liquid ammonia sample prior to passing through the metering valve. Note: Total vaporization is the key to the technique, since it is critical that all species in the liquid phase be volatilized and remain in the vapor phase in order for quantitative measurement to be valid. With total vaporization, the gas composition that enters the FTIR thus represents the liquid phase composition of the ammonia cylinder.

Instant and complete vaporization was insured by providing a large heated surface area for relatively small flow rates of only 1–2 slpm and was indicated by very stable moisture readings with fluctuations <3–5%. Even though ammonia is completely vaporized by the time it reaches the sampling cell due to its high vapor pressure, partial vaporization in the vaporizer may occur if the temperature is not well controlled. Fluctuating moisture residuals in the lines and strong cooling and moisture condensation at the needle valve from Joule-Thomson cooling or vaporization of residual liquid causes fluctuations as high as 50% in moisture readings that are easily detectable.

The stability of the moisture measurements and, therefore, the accuracy strongly depended on the stability of the temperature and pressure inside the sample cell. It was crucial that all gas-line segments and regulators exposed to ammonia gas under cylinder pressure were heated above room temperature (typically 50–70°C) during sampling to allow precise temperature control and prevent spurious condensation of ammonia.

Safety Considerations

To ensure safe operation, the system was installed in a walk-in hood. Check valves were used on all purge lines to prevent accidental back streaming of ammonia into the nitrogen lines. The ammonia exhaust lines were vented into a scrubber that was filled with H_2SO_4 solution sized for catastrophic containment. Ammonia sensors in the hood and at the scrubber exhaust line were connected to an alarm system that allowed early detection of an accidental release or exhausted scrubber solution.

Calibration and Data Analysis

To ensure accurate calibration over a broad concentration range, a dynamic dilution manifold was specially constructed to allow generation of standard moisture challenges in an ammonia matrix. The dilution system, shown in Fig. 2, consisted of four mass flow controllers with all metal components (Model 1679, MKS Instruments, Andover, MA), two Nupro back-pressure regulators, two pressure gauges, and one custom-made 10 ml glass diffusion vial that was housed in a thermostated stainless-steel vessel. The manifold components were connected with 1/8″ electropolished 316 stainless steel lines using all-metal VCR fittings. All lines were minimized to reduce dead-space and surface area, and they were also heated to limit adsorption and out-gassing of water vapor from the surfaces. The manifold was tested with a Veeco MS-170 helium leak detector (Veeco

Table I. Gas-Phase versus Liquid-Phase Moisture Concentration in Ammonia Cylinders*

Cylinder	Contents (kg of NH_3)	Gas Phase Moisture** (ppm)	Liquid Phase Moisture (ppm)	Liquid/Gas Moisture
	13.62	~ 20	628 ± 8	31
	0.61	~ 21	297 ± 5.3	14
	22.72	~ 2.03	143 ± 1.9	72
	15.45	~ 0.55	148 ± 1.6	270
	15.45	~ 8.9	70.7 ± 0.8	8
	22.72	~ 1.9	64.2 ± 0.8	34
	6.81	< 0.1	2.9 ± 0.23	>30
	22.72	n/a	0.2	n/a

*Flow rate: 0.8 slpm, cell pressure: ambient, cell temperature: 323.2 K.
**Minimum value reached during measurement, see text.

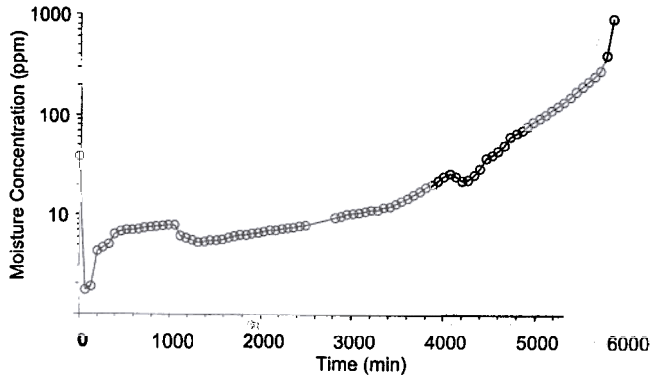

Fig. 7. Gas phase moisture concentration during complete consumption of a cylinder of ammonia. Flow rate: 5.2. slpm, initial liquid phase moisture: 38 ppm.

Instruments, Plainview, NJ) and found to be leak-free (leak rate < 10^{-11} cm^3/min).

In the first stage of the calibration manifold, the diffusion vial was maintained under purified nitrogen flow at constant pressure, temperature, and flow rate. The weight loss of the diffusion vial was frequently verified and used to calculate the moisture concentration in the wet nitrogen stream. In the second stage of the manifold, a small fraction of the wet nitrogen stream was introduced into an ammonia stream that was dried to below the detection limit of the FTIR using a Nanochem OMA purifier designed for use with NH_3 (Semi Gas Systems).[7] For each calibration point generated, the concentration of moist nitrogen in the ammonia matrix did not exceed 10% by volume. The concentration of moisture in the ammonia was adjusted by changing either the temperature of the moisture source, the ratio of wet nitrogen to dry ammonia, or the dilution flow rate of the moisture source.

A classical least-squares (CLS) method from Nicolet's *OMNIC QuantPad* software was used for data analysis and applied to apodized spectra. The CLS method mathematically combines calibration spectra for moisture in nitrogen and ammonia to match the sample spectra and calculates the actual concentration from the individual contributions of the calibration spectra. This method potentially can analyze several components simultaneously and the residual spectra yield information of additional impurities that might not have been accounted for. The algorithm requires the selection of spectral regions where the different compounds have the least interference. Several spectral windows between 3682 and 3988 cm^{-1} were used for this work. Figure 3 shows a typical calibration curve that covers a concentration range between 0 and 151 ppm. A second order polynomial correction was used to account for deviations from Beer's law, which are assumed to be a result of the low spectral resolution of 4 cm^{-1} used for all measurements.[17] The stability of the moisture readings at low concentration gives a limit of detection (LOD) of <45 ppb based on 3σ calculated from signal/noise ratios. This number, however, does not represent the absolute accuracy of the method based on the calibration data used, and a method detection limit (MDL) is preferred. MDLs were calculated using linear regression analysis at 99.87% confidence according to the method of Bzik et al.[18] This method takes into account variances of the calibration system as well as changes in the bench moisture background and reproducibility of blanks. The MDL for the experiments reported here was ~0.36 ppm over the range 0–50 ppm, and 0.15 ppm over the range 0–10 ppm. Incorporation of higher concentrations into the MDL calculations leads to higher detection limits because of the larger absolute error associated with the higher concentration measurement. Under optimal conditions and low calibration ranges, MDLs as low as <10 ppb have been reported with a similar setup utilizing an InSb detector.[15] Such low MDLs were not required for the scope of this work.

RESULTS AND DISCUSSION

Gas-Phase Sampling

Commercial ammonia is supplied as a liquefied gas at room temperature. Depending upon size, a cylinder can contain 0.5 to 150 kg of ammonia, most of it in the liquid phase. Liquefied gases are usually sampled for volatile impurities by gas-phase analysis, a procedure in which the gas in the headspace of the cylinder is drawn off under natural pressure (114 psig at room temperature). Figure 4 shows a typical measurement of moisture in ammonia by gas-phase sampling at 2 and 6 slpm. Usually, the observed moisture level dropped rapidly to a minimum and rose again. The time required to observe increasing moisture after an initial drop ranged anywhere from a few minutes to several hours. Moreover, the shape of the moisture curve was highly variable, so that neither the time nor the moisture level of the minimum was reproducible from sample to sample.

In addition to variability over time, the gas-phase

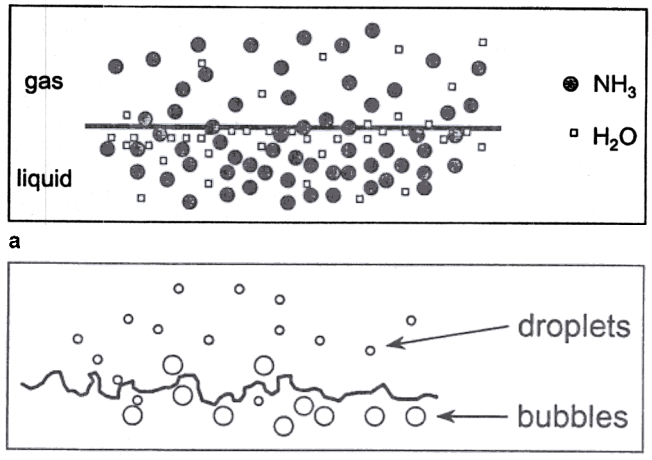

Fig. 8. Qualitative model of moisture partitioning under flow conditions: (a) surface enrichment of moisture caused by selective evaporation of ammonia, (b) droplets transport moisture into the gas phase during violent boiling.

measurements showed marked sensitivity to flow rate. Figure 5 shows changes in gas-phase moisture as a function of flow rate from a cylinder containing 127 ppm moisture in the liquid phase (see below). The increase in moisture over time during gas phase sampling was generally more rapid at higher flow rates. The effect of stirring by agitation of the cylinder can also be seen in Fig. 5. Agitation of the cylinder temporarily caused the moisture levels to drop significantly.

Liquid-Phase Sampling

Liquid sampling produced a markedly more stable result than gas-phase sampling. The liquid-phase moisture level of a given sample cylinder was considerably higher than the gas-phase moisture level, and was always very stable over long time periods and independent of the flow rate. Figure 6 shows a typical moisture measurement by liquid-phase sampling at a flow rate of 2 slpm over a period of 140 min. The moisture concentration in this particular cylinder was 96.7 ppm ± 1.4 ppm.

Several ammonia cylinders of different sizes from different vendors were analyzed via gas-phase and liquid-phase sampling, and the results are summarized in Table I. In each case, the minimum gas-phase level reached is the value that is reported for gas-phase sampling, although as discussed above, this value is highly variable. Table I demonstrates the wide range of different liquid-phase moisture concentrations that were encountered during this study, along with the lack of clear correspondence between gas-phase and liquid-phase moisture levels.

Gas-Phase Moisture Variation over the Life of a Cylinder

A cylinder with 38 ppm moisture in the liquid phase was completely vented through the FTIR at 5.2 slpm to determine the changes in moisture concentration over the lifetime of a cylinder under 'real-world' operating conditions (Fig. 7). The observed behavior is similar to measurements reported for other condensable gases such as HCl.[19] The gas-phase moisture increased steadily throughout the duration of the experiment. Approximately 10% of the total moisture content was released over the first 2/3 of the cylinder lifetime. The remaining 90% evolved mostly at the end of the experiment when moisture levels increased to approximately 1100 ppm. The integrated amount of moisture measured over the lifetime of the cylinder was very close to the expected value based upon the liquid-phase measurement of 38 ppm.

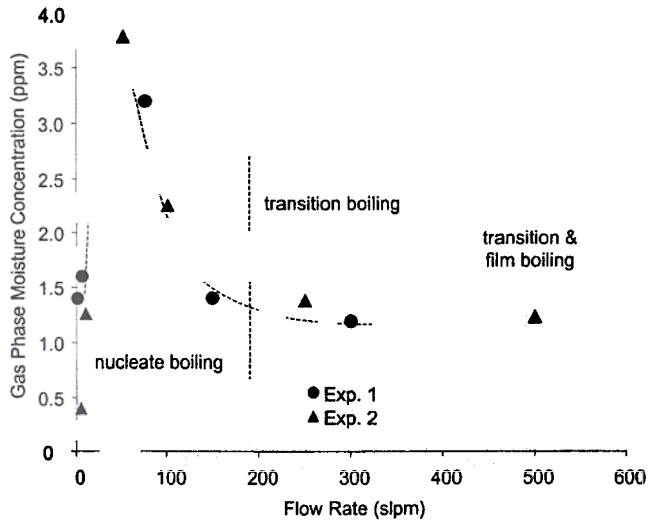

Fig. 9. Gas phase moisture concentration as function of boiling mechanism in bulk ammonia container.[22]

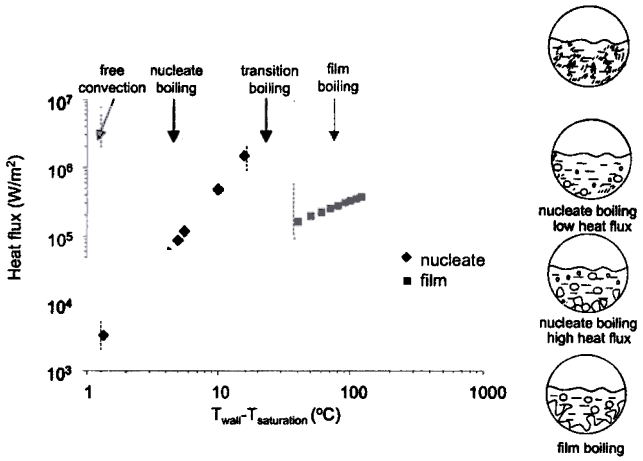

Fig. 10. Calculated boiling regimes for an ammonia cylinder and different boiling mechansims.

Qualitative Model of Evaporation of Ammonia/Water

The instability of the moisture level in the gas phase of an ammonia cylinder over time is a phenomenon that is qualitatively reproducible, although highly variable from sample to sample. Clearly, evaporation of the liquid phase of the ammonia/water system inside the cylinder is a non-equilibrium process. The dependence of moisture level upon flow rate and the sudden drop in moisture produced by mixing also point to non-equilibrium gas flow. No quantitative model for the observed behavior is currently available. However, we wish to propose a qualitative model based on transport limitations at the gas/liquid interface.

The volatility of ammonia is more than two orders of magnitude higher than that of water. The vapor pressure of water at room temperature (20°C) is 0.00235 MPa whereas ammonia has a vapor pressure of 0.862 MPa.[20] Gas and liquid phase are expected to be in thermodynamic equilibrium during storage of the cylinder. When the cylinder valve is initially opened, a flow of 'true equilibrium gas' is expected for some short time. Ammonia, however, evaporates at a much higher rate than water based on its higher volatility. Therefore water is enriched at the surface over time as illustrated in Fig. 8a. The moisture content of the evaporating ammonia depends on the liquid composition at the surface and therefore will

increase if no effective mixing process with the bulk phase is present. The only mixing processes operating within a stationary cylinder are a) diffusion and b) convection due to temperature gradients caused by evaporative cooling of the ammonia surface. However, these processes are slow compared to evaporation. The model of a water-enriched surface layer also accounts for the observed drop in gas-phase moisture after agitation of the cylinder, a process that would mix the moisture-rich surface layer with the bulk liquid to obtain uniform liquid composition.

Other factors that might interfere with a diffusion-limited evaporation model must be considered. It is known that boiling will occur in condensable gases when large flow rates cause a pressure drop in the cylinder head space.[21] As illustrated in Fig. 8b, liquid aerosol particles can be formed by bursting bubbles, and can then be carried along with the vapor stream. These aerosol particles might contain water at levels similar to the liquid composition and therefore result in gas moisture concentrations downstream that are significantly higher than expected based on vapor/liquid equilibrium. Different types of boiling mechanisms can be observed, dependent on the temperature gradient between cylinder wall and the liquid phase. Continuous flow causes increased temperature gradients by evaporative cooling of the liquid. The amount of bubbles formed, and the number of corresponding aerosol particles, are expected to change with changing boiling mechanism. Moisture concentrations initially increase with increasing flow rate, reach a maximum, and then drop as the flow is further increased, as shown in Fig. 9, for a bulk ammonia container.[22] The different boiling mechanisms can be correlated to the heat transport from the ambient surrounding into the cylinder. Figure 10 illustrates the heat flux as a function of the temperature gradient from the cylinder wall to the bulk liquid phase based on calculations using the empirical Kutateladze equation.[23] When the temperature gradient is small, free convection currents are the determining factor

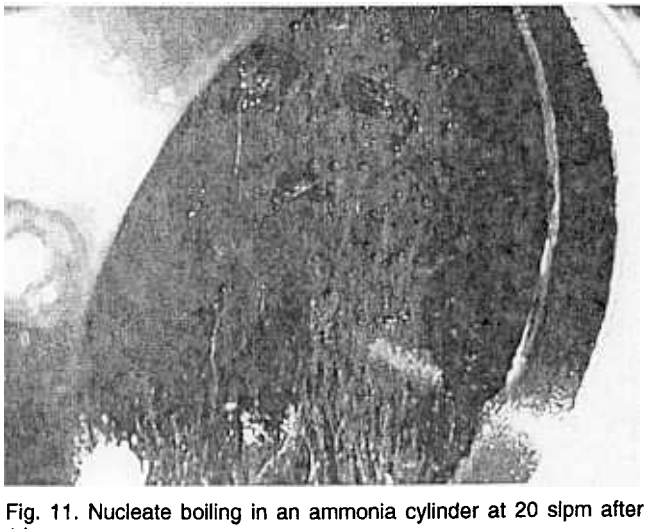

Fig. 11. Nucleate boiling in an ammonia cylinder at 20 slpm after 1 hour.

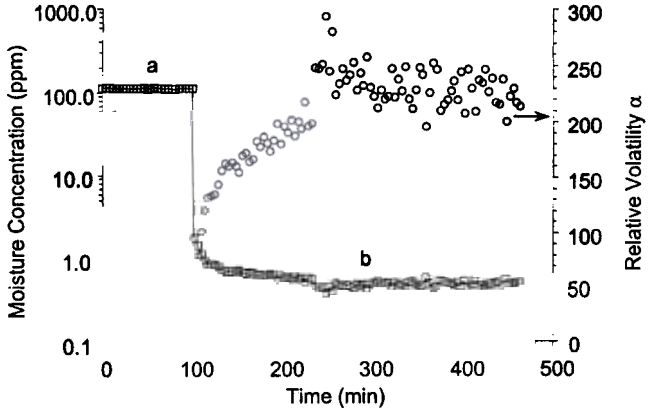

Fig. 12. Measurement of moisture in liquid ammonia and gas phase ammonia under "quasi static" conditions and relative volatility $\alpha = (x_{H_2O}y_{NH_3})/(y_{H_2O}x_{NH_3})$ at room temperature liquid phase; b) vapor phase.

for heat transfer from the cylinder surface to the liquid phase. As the gradient increases, nucleate boiling, indicated by bubble formation on the cylinder surface, causes increasing heat flux due to increased mixing efficiency. The stage where the moisture maximum is observed in Fig. 9 corresponds to the nucleate boiling phase. After the transition boiling, the system eventually reaches the film boiling stage, a condition where the cylinder walls are sufficiently warm compared to the bulk liquid that a vapor film completely covers the walls and prevents liquid contact. Heat transport through the vapor film is slow, and the violence of the boiling process actually decreases again.

The different boiling regimes for ammonia were confirmed by visual observation using a cylinder equipped with a sight glass. Figure 11 shows a photograph of boiling liquid ammonia inside the cylinder after maintaining a flow of 20 slpm for 1 hr, corresponding to violent nucleate boiling. As the temperature difference between the cylinder wall and content approaches ~15°C, transitional boiling was observed with decreasing bubble formation and gas phase moisture.

Temperature data were recorded both at the center and the outside surface of the cylinder to confirm the onset of different boiling mechanisms. A custom heat transfer model that will be the subject of a future publication[24] was used to estimate the temperature profile inside the cylinder. The comparison of the data with model predictions showed that the model predicts the temperature in a cylinder within ±0.6°C. Estimating the temperature profile is essential for the prediction of the boiling mechanism and the time of equilibration for the moisture concentration.

Another factor that cannot be addressed easily is the amount of moisture adsorbed on the cylinder walls. Different surface area and chemical composition of the walls are expected with different cylinder materials and preparation procedures and might cause significantly different contributions to the observed moisture levels.

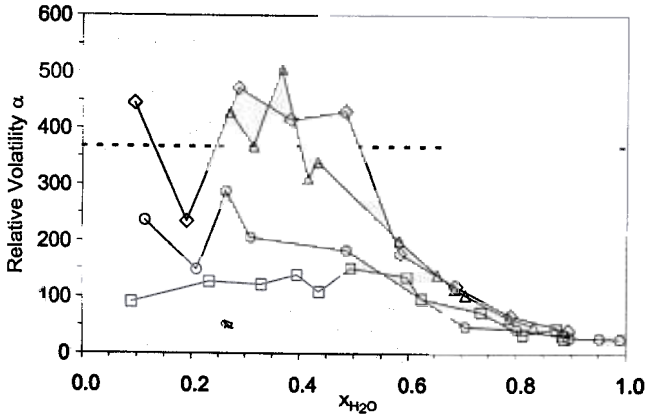

Fig. 13. Relative volatilities a = ($x_{H_2O}y_{NH_3}$)/($y_{H_2O}x_{NH_3}$)calculated from literature data. (□) ~ 305 K (23); (◇) 294.3 K (22); (○) 313.2 K (21); (Δ) 293.2 K (24); (- - -) 293.2 K (Raoult's Law).

Thermodynamic Equilibrium Measurements

Vapor-liquid equilibrium data can provide information about the lowest moisture levels that can be expected in the gas phase at a given liquid composition. Experiments to determine phase equilibria are usually performed under static conditions to allow complete equilibration. Static FTIR measurements at the ppm and ppb level were attempted using a standard 10 m path length cell that was partially filled with liquid ammonia. These measurements were not successful due to high noise levels, apparently caused by fluctuations in the refractive index of the gas phase due to convection. (The end of the White cell that is inside the spectrometer is slightly higher in temperature than the other end because of heat evolved by nearby electronic components in the spectrometer bench.)

An alternative 'quasi-static' approach was used to obtain an approximation of the equilibrium concentration of gas phase moisture above a liquid phase of known moisture content. An ammonia cylinder containing approximately 300 g of liquid ammonia and 49 l ammonia in the gas phase (~180 g) was inverted according to Fig. 2. After thoroughly shaking the cylinder and then equilibrating for 48 hr at room temperature, it was assumed that the gas and liquid phases were in thermodynamic equilibrium.

The liquid-phase ammonia was then sampled at 1 slpm to determine a liquid concentration of 113 ± 1.3 ppm moisture. The gas phase was not disturbed significantly during these measurements since only a small volume of liquid (about 0.1% of the total volume) was removed from the cylinder. After the liquid-phase measurements, the cylinder was emptied slowly. At the point where all liquid was removed, the cylinder flow was stopped and the FTIR sampling system was dried with Nanochem-purified ammonia to remove residual moisture left by the liquid sampling procedure.

The cylinder flow was then resumed at 1 slpm and the gas phase remaining in the cylinder (assumed to be essentially the same composition as when it was in equilibrium with the liquid phase) was sampled. Unlike previous gas-phase measurements, the moisture readings in this experiment were steady during sampling, presumably because no liquid ammonia was present that could evaporate and cause changes in the composition. The cylinder pressure continuously dropped from 0.862 MPa (the equilibrium pressure when the last liquid was removed at room temperature) to approximately ambient pressure where flow could no longer be sustained. Figure 2 shows the results of this measurement. The gas-phase moisture concentration was 0.5 ± 0.03 ppm. It cannot be ruled out that moisture adsorbed to the wall of the cylinder contributes to the gas-phase moisture concentration, since the pressure change during gas sampling might have shifted the adsorption equilibrium of moisture on the cylinder walls. However, this effect is likely to be minor since a stable moisture reading was established.

The liquid and gas moisture concentrations (x_{H_2O}/y_{H_2O}) obtained from the quasi-static measurement can be used to calculate the relative volatility of water to ammonia, $\alpha = (x_{H_2O}\, y_{H_2O})/(y_{H2O}x_{NH3})$ of 227 ± 15 at room temperature (see Fig. 12). At moisture concentrations in the low ppm range, x_{NH_3} and $y_{NH_3} \rightarrow 1$ and $\alpha \rightarrow x_{H_2O}\, y_{H_2O}$. This value is substantially higher than most of the nominal values calculated from measurements at 0.8 slpm except for cylinder 4 in Table I, a result that illustrates again the strong flow-rate dependence upon the moisture level in gas-phase measurements. Several theoretical approaches,

Table II. Extrapolated Relative Volatilities at 100 ppm Moisture in the Liquid Phase

Source	T (K)	Relative Volatility	Lowest x_{H_2O} Measured	Comments
(28)	293.2	~402	0.272	P, T, x, y measured
(26)	294.3	~399	0.0949	P, T, x, y measured
(27)	~305	~118	0.0915	P, T, x, y measured
(25)	313.2	~212	0.115	P, T, x, y measured
Redlich-Kister Eq.	293.2	~295	—	Parameters fitted to (26)
SRK EOS	293.2	1240	—	Binary Parameters from (30)*
Raoult's Law	293.2	~370	—	Calculated (20)

*Calculations performed with HYSYS Simulation Package, Hyprotech Ltd.

such as equations of state and activity coefficient models, were investigated to extrapolate from literature vapor-liquid-equilibrium data of the NH_3/H_2O system that were available near room temperature[25–28] to the concentration range of interest for this study (Fig. 13). The lowest concentrations typically measured in the liquid phase were in the range of $x_{H_2O} \geq 0.1$ (≥100,000 ppm). Figure 13 also illustrates the wide scatter of the experimental data especially at low moisture concentrations. The reliability of the different data sets is discussed thoroughly in Ref. 29. The magnitudes of the relative volatilities calculated from individual sets of experimental data in the literature did not change significantly throughout the measured concentration range in the ammonia-rich region. Averaging of the relative volatilities in the low concentration region as an estimate for the behavior at 100 ppm liquid-phase moisture, therefore, appears to be justified. Table II lists the average relative volatility calculated from the different sets of experimental data displayed in Fig. 13. The accuracy of theoretical approaches, such as equations of state or activity coefficient models, is usually strongly dependent on the availability and reliability of experimental data for adjustments of the model parameters. The extrapolation beyond the range of measured data, therefore, is often not very reliable. For example, relative volatilities of ~1240 were calculated with the Soave-Redlich-Kwong equation of state (SRK EOS) using binary-interaction parameters that are available in literature.[30] Equations of state are usually adjusted to describe a wide concentration and temperature range, which can result in compromised accuracy at extreme conditions such as the range of low water concentrations. Activity-coefficient models are expected to be more reliable in a complicated system such as NH_3/H_2O. Extrapolation to low water concentrations using a four-parameter Redlich-Kister activity coefficient equation[31] and assuming ideal gas-phase behavior yield relative volatilities close to 300. A simple approach based on Raoult's Law ($P_{total} = P_{vap-NH_3}x_{NH_3} + P_{vap-H_2O}x_{H_2O}$; P_{vap-NH_3} and P_{vap-H_2O} are the pure compound vapor pressures of ammonia and water)[20] resulted in a value of ~370 at room temperature. The results of the model extrapolations are also listed in Table II. The values calculated by Raoult's law and the activity-coefficient models are reasonably close to the observed quasi-equilibrium value of 227, which indicates that the system does not deviate strongly from an ideal solution at low water concentrations. However, the large uncertainty in the extrapolation, as well as the limit of the experimental method, should be taken into account when considering the absolute accuracy of the measured number.

CONCLUSION

Under static conditions, moisture in liquefied gases such as ammonia, thermodynamically equilibrates between the liquid phase and the head space. Quasi-static measurements and thermodynamic calculations indicated partition coefficients between liquid- and gas-phase moisture of ~ 200. Under flow conditions that require vaporization from the liquid phase, the equilibrium is disturbed significantly by mass transport limitations, temperature changes due to thermal losses from the required heat of vaporization, and mechanical disturbances from boiling processes. The disturbed equilibrium results in dramatic changes of the moisture concentration in the gas phase withdrawn from the cylinder dependent on the operating conditions. The true moisture content of a cylinder can be determined more reliably by the liquid-phase concentration that can be measured easily by analyzing completely vaporized sample streams withdrawn from the liquid phase. FTIR was used as a method of choice for this work due to its high sensitivity and reliability even in manufacturing environments.

REFERENCES

1. R.W. Shrewsbury and J.F. Salfelder, *Microelectronic Manufacturing and Testing* 9, 13 (1986).
2. G. Vergani, M. Succi, E.J. Thrush, J.A. Crawley, W. Van der Stricht, P. Torres, and U. Kroll, *Proc. of the 43rd Annual Technical Meeting of the Inst. of Enviro. Sci.* (Mt. Prospect, IL: Inst. Enviro. Sci., 1997), pp. 262–272.
3. S. Monroe, *J. Inst. Enviro. Sci.* 41, 21 (1998).
4. M.I. Toth, D.A. Zatko, D.F. Yesenofski, M. Schneegans, and J. Helneder, *MICRO* 7,79 (1997).
5. J. Wei, J. Pillion, and C. Hoang, *J. Inst. Enviro. Sci.* 41, 43(1997).
6. *SEMI,* Standard C3.12-94 (Mountain View, CA: Semiconductor Equipment and Materials International, 1996).
7. S.-Q. Wu, J. Morishita, H. Masusaki, and T. Kimishima, *Anal. Chem.* 70, 3315 (1998).
8. R. Kastle, R. Grisar, M. Tacke, D. Dornisch, and C. Scholz, *Microcontamination* 11, 27 (1991).
9. J.-M. Girard and P. Mauvais, *Proc. 5th Int. Symp. on Semicond. Mfg.* (Tokyo: The Ultraclean Soc., 1996), pp. 325–328.
10. J.B. Goddard, *A History of Gas Analysis* (New York: Wiley-VCH, 1997), pp. 4–5.
11. P.R. Griffiths and J.A. de Haseth, *Fourier Transform Infrared Spectroscopy* (New York: John Wiley & Sons, 1986).
12. K. Miyazaki, Y. Ogawara, and T. Kimura, *Bulletin of the Chem. Soc. of Jpn.* 66, 969 (1993).
13. B.R. Stallard, L.H. Espinoza, and T.M. Niemczyk, *Proc. 41st Annual Tech. Mtg. Inst. Enviro. Sci.* (Mt. Prospect, IL: Inst. Enviro. Sci., 1995), pp. 1–8.
14. D.E. Pivonka, *Appl. Spectroscopy* 45, 597 (1991).
15. S. Salim and A. Gupta, *Proc. Clean Rooms '96* (Nashua, NH: Penn Well Publishing, 1996), pp. 22–32.
16. S. Salim, M.M. Litwin, and J.P. Natwora, Jr., *Proc. of Semicon West* (San Jose, CA: Semicond. Equip. Mater. Int. (SEMI), 1998), pp. 1–17.
17. P. Jaakkola, J.D. Tate, M. Paakkunainen, J. Kauppinen, and P. Saarinen, *Appl. Spectroscopy* 51, 1159 (1997).
18. T.J. Bzik, G.H.J. Smudde, D.A. Zatko, and J.V. Martinez de Pinillos, *Limit of Detection* (New York: Wiley-VCH, 1996), pp. 163–196.
19. E. Flaherty, C. Herold, J. Wojciak, D. Murray, A. Amato, and S. Thomson, *Solid State Technol.* (1987), pp. 69–75.
20. R.C. Reid, J.M. Prausnitz, and B.E. Poling, *The Properties of Gases and Liquids,* 4 ed. (New York: McGraw-Hill, Inc., 1987).
21. H.-C. Wang, R. Udischas, and B. Jurcik, *Proc. 43rd Annual Tech. Mtg. Inst. Enviro. Sci.* (Mt. Prospect, IL: Inst. Enviro. Sci., 1997), pp. 6–12.
22. B. Yücelen, J. Vininski, and R. Torres, *Proc. Semicon West* (San Jose, CA: Semicond. Equip. Mater. Int. (SEMI), 2000), pp. A1–A6.
23. A. Arkhrov, I. Marfenina, and Y. Mikulin, *Theory and Design*

of Crygenic Systems (Moscow: Mir Publishers, 1981), pp. 384–391.
24. B. Yücelen, J. Vininski, and R. Torres, to be submitted to the *J. Electron. Mater.* (2001).
25. P.C. Gillespie, W.V. Wilding, and G.M. Wilson, *Research Report No. 90* (Provo, UT: Gas Processors Association, 1985).
26. R.A. Macriss, B.E. Eakin, R.T. Ellington, and J. Huebler, *Res. Bulletin No. 34* (Chicago, IL: Inst. of Gas Technol., 1964).
27. S.S.H. Rizvi and R.A. Heidemann, *J. Chem. and Eng. Data* 32, 183 (1987).
28. T.A. Wilson, *Bulletin No. 146* (Urbana, IL: Univ. of Illinois, 1925) pp. 45–61.
29. R. Tillner-Roth and D.G. Friend, *J. Phys. and Chem. Ref. Data* 27, 45 (1998).
30. L. Oellrich, U. Plöcker, J.M. Prausnitz, and H. Knapp, *Int. Chem. Eng.* 21, 1 (1981).
31. J.M. Prausnitz, R.N. Lichtenthaler, and E.G. de Azevedo, *Molecular Thermodynamics of Fluid-Phase Equilibria,* 2nd ed. (Englewood Cliffs, NJ: Prentice-Hall, 1986).